Water Science & Technology

Water Science & Technology Vol 87 No 4, 924 doi: 10.2166/wst.2023.032

Electro-Fenton mineralization of real textile wastewater by micron-sized ZVI powder anode

Wenjuan Xue[a], Xiaoting Hong [a,*], Yingying Du[a] and Bin Chen[b]

[a] Department of Chemistry, School of Science, Zhejiang Sci-tech University, Hangzhou 310018, P. R. China
[b] Zhejiang Agriculture and Forestry University, Lin'an 311300, China
*Corresponding author. E-mail: hongxt@zstu.edu.cn; hanren.xiaoting@gmail.com

XH, 0000-0002-2420-4257

ABSTRACT

The diverse compositions and complex nature of the textile wastewater make it imperative to find an economical and suitable degradation pathway. The degradation of real textile wastewater on a novel heterogeneous electro-Fenton system was carried out with a composite anode of magnetically fixed micron ZVI coupling with a Ti/RuO_2-IrO_2 sheet. The influences of different variables such as mZVI dosage, H_2O_2 amount, applied voltage and pH value on both total organic carbon and chemical oxygen demand removal efficiencies and energy consumption were investigated. The optimized parameters were simultaneously verified by using electrochemical workstation Tafel curves and Nyquist plots. The optimal operating conditions for evaluating the wastewater treatment were H_2O_2 dosage of 0.10 mol·L^{-1}, applied voltage of 5.0 V, mZVI amount of 1.0 g·L^{-1} and initial pH value of 3.0. The high TOC and COD removal efficiencies of 92.44 and 82.84% could be achieved simultaneously in 60 min, respectively. XRD, XPS and SEM-EDS were used to investigate the interaction between the pollutant and the mZVI. GC-MS analysis was performed on untreated and treated wastewater to determine the degradation of pollutants in dyeing wastewater during the electro-Fenton process and to effectively propose a suitable degradation mechanism for this system.

Key words: AOPs, degradation, electro-Fenton process, textile wastewater

HIGHLIGHTS

- A heterogeneous electro-Fenton process was performed on mZVI anode.
- This study is performed on the real textile wastewater.
- High COD and TOC removal efficiencies were achieved by the heterogeneous E-Fenton process.
- The performance of electro-Fenton for contaminant removal was evaluated at different parameters.
- The mechanisms were proposed based on the physiochemical and electrochemical properties of the anode.

GRAPHICAL ABSTRACT

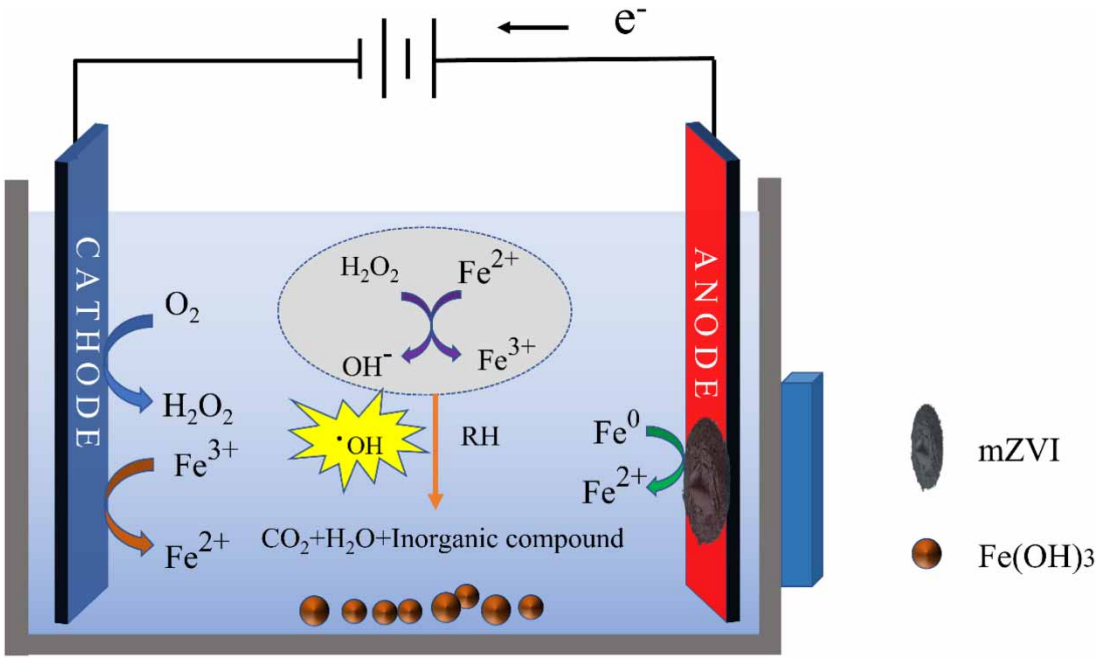

1. INTRODUCTION

In recent years, considerable amounts of wastewater with significant organic carbon levels have aroused a widespread concern of the whole society. Among them, the discharge from the textile factory is a significant pollution source. According to statistics, the amount of wastewater from textile enterprises in China is as high as 4 million tons per day (Bilińska *et al.* 2017). However, the wastewater contains various organic pollutants with high concentrations and some heavy metals (Yamjala *et al.* 2016) due to the numerous chemicals used in the textile dyeing process. In addition to the complex chemical structures, other different characteristics of dyestuffs such as photo-resistance, biodegradation resistance, variable pH, carcinogenicity and mutagenicity make textile wastewater even more difficult to properly be treated (Nidheesh & Gandhimathi 2012; Naje *et al.* 2017). Therefore, it is imperative to explore better, more energy-saving and inexpensive technology for the degradation of textile effluent.

The conventional treatment options mainly include biological and physico-chemical processes (Khlifi *et al.* 2010; Samuchiwal *et al.* 2021). Although biological treatment is quite economical and eco-friendly, the long treatment cycle is an important shortcoming. Moreover, dyes have complex aromatic structures, which can produce carcinogenic, toxic and mutagenic aromatic amines if the dyes are decomposed by anaerobic microorganisms (Sarikaya *et al.* 2012; Yamjala *et al.* 2016; Paz *et al.* 2017). Additionally, textile wastewater includes non-biodegradable and refractory dyes indicating a low biodegradation index, which further leads to typical biological treatment inefficiencies (Somensi *et al.* 2010; Nakhate *et al.* 2019). Chemical removal (Bahadur & Bhargava 2019), nanofiltration adsorption (Chen *et al.* 2015) and other physico-chemical approaches also have their own drawbacks. They often encounter problems such as high-cost, failure to meet discharge limits and membrane fouling. Recently, advanced oxidation processes (AOPs) have attracted the great attention of many researchers because of their high effectiveness and mineralization efficiency (Dolatabadi *et al.* 2021; Li *et al.* 2021). Hydroxyl radical has a significant impact on the AOPs. Its redox potential (2.80 V) is much larger than those of typical oxidants such as potassium permanganate or hydrogen peroxide, and also more efficient than radical-based oxidants such as $SO_4^{-}\bullet$ (2.60 V) (Ileri & Dogu 2022). Fenton (Sayin *et al.* 2022), O_3 processes (Bilinska *et al.* 2020), peroxides (Chow & Leung 2019), methods based on ultraviolet light or ultrasonic decomposition (Cai *et al.* 2016), photocatalytic oxidation (Ju *et al.* 2022) and processes in which multiple methods are synergistic with each other are all AOPs (Huang *et al.* 2020; Pan & Qian 2022). Among many AOPs, electro-Fenton has extremely attractive advantages in treating hard-to-degrade wastewater due to its high oxidation capability, low

installation cost, and high efficiency as shown in the following equations.

$$Fe^0 \rightarrow Fe^{2+} + 2e^- (E^0 = -0.44\ \text{V}) \quad (1)$$

$$O_2 + 2H^+ + 2e^- \rightarrow H_2O_2 \quad (2)$$

$$Fe^{2+} + \cdot OH \rightarrow Fe^{3+} + OH^- \quad (3)$$

$$Fe^{3+} + e^- \rightarrow Fe^{2+} \quad (4)$$

The *in situ* generation of hydrogen peroxide and ferrous iron in the electro-Fenton system results in high wastewater treatment efficiency compared to the routine Fenton approach. However, most of the current electro-Fenton studies are based on simulated wastewater with one or several dyes (Kenova *et al.* 2018). Therefore, extensive research is still required for the electro-Fenton application to actual industrial wastewater.

It is also well known that the choice of electrode material is closely related to the electrochemical performance of the pollutant degradation process. An application of boron-doped diamond (BDD) electrode has shown excellent electrochemical stability in wastewater treatment. However, BDD electrodes are high in cost (Kaur *et al.* 2018). Dimensionally stable anode (DSA), consisting of titanium-based metals covered with a thin conductive layer of metal oxides, have become widely used in wastewater treatment (Feng *et al.* 2016; Baddouh *et al.* 2019a; Santos *et al.* 2020). DSA-type electrodes (IrO_2 and RuO_2-IrO_2) are very effective in the degradation of pollutants (Baddouh *et al.* 2019b; Kishor *et al.* 2021; Baddouh *et al.* 2022). The degradation of 1,4-benzoquinone was carried out on Ti/IrO_2 anodes and the main mineralization step of benzene ring breakage readily occurred, although the byproduct of carboxylic acids slightly exits and ultimately transforms to non-toxic degradants (Pulgarin *et al.* 1994). Meanwhile, according to Equations (5)–(7, RuO_2-Ti electrodes have also been reported to facilitate the production of reactive chlorine species (HClO, Cl_2 and ClO^-) (Paździor *et al.* 2019). It is important to note that active chlorines (RCS, such as Cl• and ClO•) are theoretically effective oxidants for pollutants because they react with the electron-rich part through single-electron oxidation. For textile wastewater, high chlorine content is also one of its important characteristics. Therefore, RuO_2-IrO_2-Ti anodes have great potential for decolorization and degradation of dyestuffs.

$$2Cl^- \rightarrow Cl_2 + 2e^- \quad (5)$$

$$Cl_2 + H_2O \rightarrow HClO + Cl^- + H^+ \quad (6)$$

$$HClO \rightarrow H^+ + ClO^- \quad (7)$$

Zero-valent metals have a high surface activity and are one of the methods used to degrade pollutants in water sources (Fu *et al.* 2014). Among them, zero-valent iron (ZVI) with a redox potential ($E^0(Fe^{2+}/Fe^0)$) of −0.44 V found wide application as a strong reducing agent for refractory organic pollutants. Electro-Fenton with zero-valent plate may lead to severe passivation inhibiting the release of Fe^{2+} from the anodic process due to the generation of a tiny iron oxide layer on the electrode. Apparently, ZVI powder is assumed to have undergone a more convenient electrochemical corrosion into ferrous ions because of the large surface area and high reactivity in the electro-Fenton reaction.

In this study, several composite anodes were constructed by magnetically immobilized mZVI particles on RuO_2-IrO_2-Ti (RuO_2-IrO_2/mZVI-Ti) and graphite was utilized as the cathode in this electro-Fenton process. They were then applied to the treatment of actual textile wastewater to investigate the comprehensive performance of the electro-Fenton system. The influences of several variables, such as pH, applied voltage, dosage of mZVI and concentration of H_2O_2 on its degradation capability of textile wastewater were systematically estimated from the aspect of COD and TOC removal rates. The physicochemical characteristics of the reactant precipitates and mZVI electrochemical behaviors were studied to strengthen mechanism research by electrochemical impedance spectroscopy (EIS), Tafel curves, X-ray diffraction (XRD) and X-ray photoelectron spectroscopy (XPS), scanning electron microscopy-energy dispersive spectrometry (SEM-EDS), respectively. The possible organic dyes present in the raw wastewater along with the final intermediates were evaluated by gas chromatography-mass spectrometry (GC-MS), and finally, the degradation mechanism was proposed.

2. EXPERIMENTALS AND CHARACTERIZATIONS

2.1. Wastewater sample and chemicals

The textile wastewater used in the study was collected from a textile company in Shaoxing, Zhejiang Province. The wastewater solution was preserved at 4°C before further analysis. Due to the good electrical conductivity of the wastewater sample, no additional electrolyte was required for electrochemical treatment. The characteristics of the textile wastewater are listed in Table S1.

All reagents used in the experiments were analytically pure. Micron ZVI powder (>99.9%) was purchased from Qinghe Chuanjia Welding Material Corporation (Xingtai, China). Ti/RuO_2-IrO_2 plates and graphite flakes were purchased from Schultech Industrial Technology (Suzhou, China) and Baofeng Graphite Co (Qingdao, China). The mass ratio of IrO_2 to RuO_2 coated on the titanium plate is approximately 3:8. The initial pH of wastewater solution was regulated by H_2SO_4 (1 M) and NaOH (3 M) during this experiment.

2.2. Experimental setup and operation

Figure S1 shows a schematic view of the experimental system. This study was carried out in a glass reaction tank (50 mm × 50 mm × 100 mm). RuO_2-IrO_2/mZVI-Ti and graphite sheet (30 mm × 100 mm × 1 mm) were utilized for the anode and cathode, respectively. mZVI powder covers an area of ~800 mm^2 (20 mm × 40 mm) on the surface of RuO_2-IrO_2-Ti electrode with a magnetic source outside the reaction tank. The total area of the electrode immersed in the wastewater was 2,100 mm^2. Both anode and cathode were immersed in the wastewater and connected by a direct current power supply (MCH, K303D-II, China) with a constant distance 20 mm. The wastewater with 200 mL in volume was adjusted to various pH levels (2.0, 3.0, 5.0 and 7.0) using 1 M H_2SO_4 solution or 3 M NaOH solution under different constant voltages (8.0, 5.0 and 3.0 V) in all batch experiments. During the reaction, water samples were extracted at the specified intervals and routinely filtered before analysis via a polytetrafluoroethylene syringe membrane filter with a pore size of 0.45-μm. All data points on the curves are the average of three tests with error bars.

2.3. Analysis and characterization

A total organic carbon analyzer (Shimadzu) was employed to determine TOC value and its removal rate was calculated using Equation (8). An appropriate amount of manganese dioxide was added to the sample at 60 °C for 30 min to remove the interference of excessive H_2O_2 on COD measurement. After filtration, COD values were determined using a rapid COD analyzer (5B-3F, Lianhua Technology Co., Ltd, China). TN and TP were analyzed with a continuous flow analyzer (AutoAnalyzer3, Germany). The content of heavy metals Sb and Cr was readily determined by graphite furnace atomic absorption spectrophotometry (AA-7000, Shimadzu). The conductivity probe (Shanghai Rex) and pH electrode (FiveEasy) were used to record the pH and conductivity of the wastewater solutions, respectively. Ferrous iron ion concentrations (DFe^{2+}) and total iron ion (TDFe) were analyzed using a O-phenanthroline spectrophotometer method (UV2600, Shimadzu, Japan). The morphology and structure of the precipitate flocs produced in the electro-Fenton system were observed by field-emission SEM (Sigma300, Zeiss, Germany) and EDS (Smart). In addition, the physical properties of crystalline flocs powders were monitored by XRD (D8 Advance diffractometer, Bruker). XPS (K-Alpha, Thermo Fisher Co., US) was performed to record the chemical valences of iron, carbon, and oxygen of the precipitate. Anodic oxidation analysis was performed by a Chi 660A electrochemical workstation (China) using EIS and Tafel analysis. Potential contaminants in the wastewater before and after the reaction were detected by GC-MS (Agilent 5977A, America) with a pressure of 100 kPa for the nitrogen carrier gas and the injector and detector temperatures of 220 and 280 °C, respectively.

$$\eta = \frac{C_0 - C_t}{C_0} \times 100\% \tag{8}$$

where η is the TOC removal efficiency; C_0 and C_t are the initial TOC concentration and final TOC concentration ($mg \cdot L^{-1}$), respectively.

The E_{EO} was used as a figure of merit to determine the electrical energy required to reduce pollutant concentrations by an order of magnitude (Bolton *et al.* 2001).

$$E_{EO}(\text{kWh m}^{-3}\text{order}^{-1}) = \frac{P \times \text{t} \times 1000}{V \times 60 \times \log\left(\frac{\text{COD}_i}{\text{COD}_t}\right)} \tag{9}$$

where P is the rated power for electro-Fenton reaction (kW); t is the reaction time (min); V is the volume of wastewater (L); COD_i and COD_t are initial and final COD concentrations ($\text{mg}\cdot\text{L}^{-1}$);

The COD removal of textile effluent was investigated using the pseudo-first-order kinetic model, as shown in the following equation.

$$\log\left(\frac{\text{COD}_i}{\text{COD}_t}\right) = kt \tag{10}$$

where k is the pseudo-first-order rate constant for the decay of the effluent COD concentration (min^{-1}).

3. RESULTS AND DISCUSSION

3.1. Influencing factors of the mZVI powder anode electro-Fenton system

3.1.1. mZVI dosage

The catalytic ferrous ions amount has a crucial influence on the degradation effect of organic pollutants in electro-Fenton reaction. The effect of mZVI loading amount on the removal rate of COD and TOC of dyeing wastewater was studied because the ferrous ion concentration is directly determined by the dosage of mZVI under other parameters unchanged. Figure 1(a) and 1(b) show the removal rates of COD and TOC increasing with the mZVI amount from 0.5 to 1.0 $\text{g}\cdot\text{L}^{-1}$ and a simultaneous increase in H_2O_2 production. The COD and TOC removal rates achieve 82.84 and 92.44% at 1.0 $\text{g}\cdot\text{L}^{-1}$, respectively. However, as the mZVI amount was further increased to 1.5 and 2.0 $\text{g}\cdot\text{L}^{-1}$, the removal rates of both COD and TOC decreased to different degrees. On the one hand, it could be caused by the lower anodic dissolution of agglomerated mZVI at the anode due to the excessive addition amount. On the other side, excessive Fe^{2+} consumes more OH· and competes with OH· for the mineralization of pollutants, resulting in a decrease in the utilization of hydroxyl radicals. Additionally, excessive iron ions form more iron sludges during the reaction process, thus causing secondary pollution and making the effluent unable to meet the discharge requirements. Therefore, the optimal mZVI loading was set to 1.0 $\text{g}\cdot\text{L}^{-1}$ in this study.

3.1.2. Hydrogen peroxide concentration

In the electro-Fenton reaction, oxygen transfers two electrons at the cathode to generate hydrogen peroxide, which reacts with divalent iron ions from mZVI electrodissolution at the anode to produce hydroxyl radicals for pollutant degradation. As shown in Figure 1(c) and 1(d), the COD and TOC removal rates were 50.98 and 56.76% without the addition of H_2O_2, respectively. The COD and TOC removal efficiencies initially enhanced as the increase of H_2O_2 concentrations because of the additional formation of OH· (Ghalebizade & Ayati 2019). The removal rates of COD and TOC reached 82.84 and 92.42% when the H_2O_2 concentration was 0.1 $\text{mol}\cdot\text{L}^{-1}$, respectively, indicating that dyeing pollutants were of high mineralization efficiencies. However, the removal rate decreased as further increase in H_2O_2 concentration to 0.15 $\text{mol}\cdot\text{L}^{-1}$ and obvious flocculent foams were observed on the surface of the wastewater. This proves that the excess of hydrogen peroxide leads to its severe self-consumption (Equation (11)) and concomitant oxygen carries the iron species-based flocs to the surface. Herein, the H_2O_2 concentration was chosen to 0.1 $\text{mol}\cdot\text{L}^{-1}$ for better utilization of hydroxyl radicals in this electro-Fenton reaction.

$$2H_2O_2 \rightarrow 2H_2O + O_2 \tag{11}$$

3.1.3. Initial pH value

Similarly, the wastewater pH has a significant impact on the electro-Fenton system, which influences the wastewater conductivity, the present form of iron species and the utilization efficiency of H_2O_2 (Naje *et al.* 2017). In this experiment, the

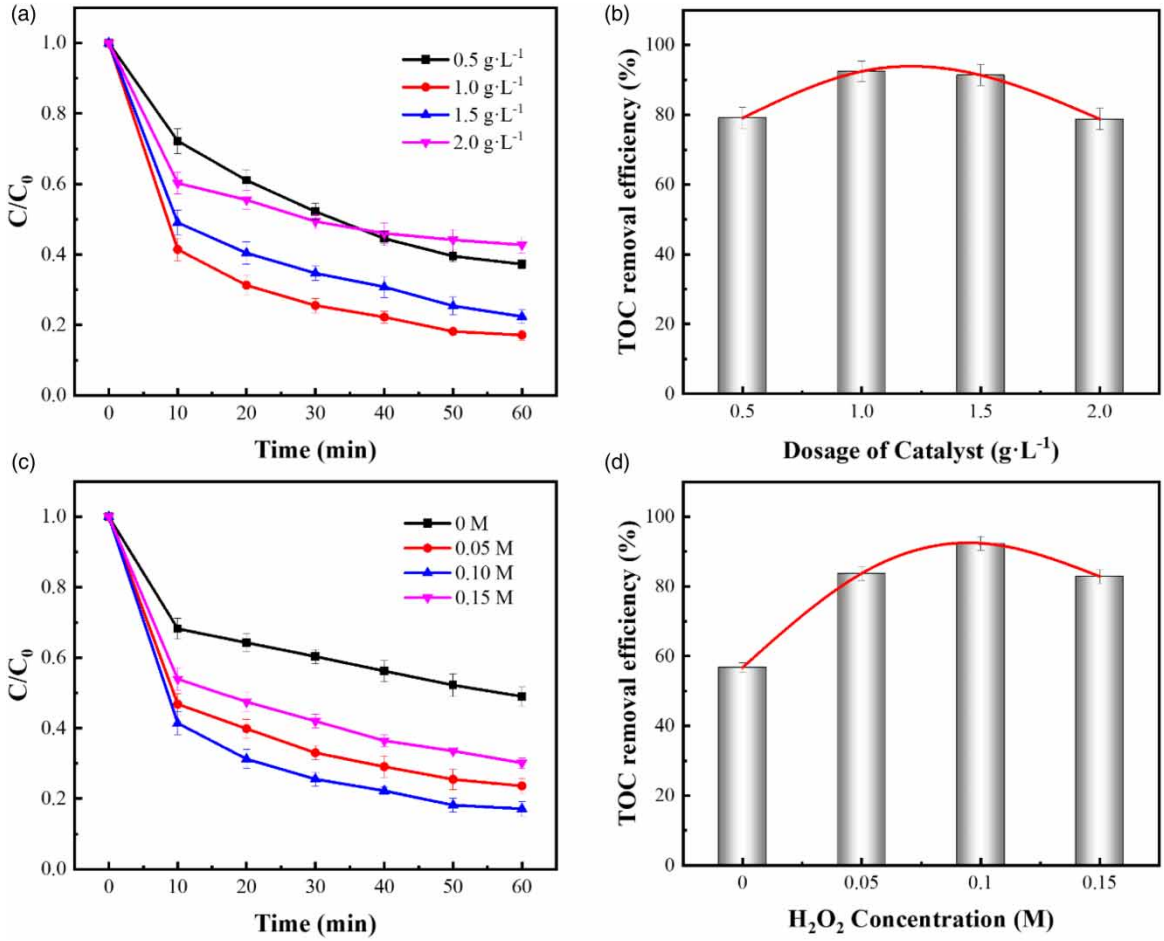

Figure 1 | Influence of mZVI dosage on (a) COD; (b) TOC removal; influence of various H_2O_2 concentrations on (c) COD; (d) TOC removal.

variation of COD and TOC of textile wastewater was studied at different initial pH values (2.0, 3.0, 5.0 and 7.0). Figure 2(a) and 2(b) shows that the COD and TOC removal rates are of the same variation trends. The removal efficiencies of the pollutants at pH of 2.0, 3.0, 5.0 were much higher than that at pH = 7.0, and a maximum removal efficiency value was observed at pH of 3.0 for this electro-Fenton reaction.

It is reported that $Fe(OH)_2$ present at pH = 3.0 has higher Fenton reaction activity than Fe^{2+} (Pignatello *et al.* 2006). However, Fe^{2+} could easily be converted to $Fe(OH)_3$ precipitates from pH value equal to 3.7 (Liu & Wang 2007). Hence, as the pH value was further increased, Fe^{2+} ions were largely converted into Fe^{3+} and further formed $Fe(OH)_3$ precipitates, thus weakening the reaction activity. An initial pH value (3.0) of wastewater was set for this study. Figure S3 reveals the pH value variation of the wastewater during the reaction. The values were kept rising as a result of the interaction between Fe^{2+} and hydrogen peroxide in 60 min; however, the overall increase degree was not significant, which could be impeded by the accumulation of carboxylic acid and CO_2 from efficient degradation of dyeing pollutants (Bakheet *et al.* 2013).

3.1.4. Applied voltage

The loaded electric field is the main dynamic force of electro-Fenton system. Normally, the higher the applied voltage, the more intense the reaction and the higher the pollutant removal efficiency. This is confirmed by results shown in Figure 2(c) and 2(d), where the COD and TOC removal efficiencies increased by 11.85 and 9.59% with the increasing voltage (3.0–5.0 V), respectively. This can be attributed to the increase in hydrogen peroxide production on the cathode surface due to the increase in current intensity (Martínez-Huitle & Brillas 2009; Khataee *et al.* 2011). However, as the applied voltage was further increased to 8.0 V, there was a slight decrease in the removal rate. The principal reason for this decrease is due to

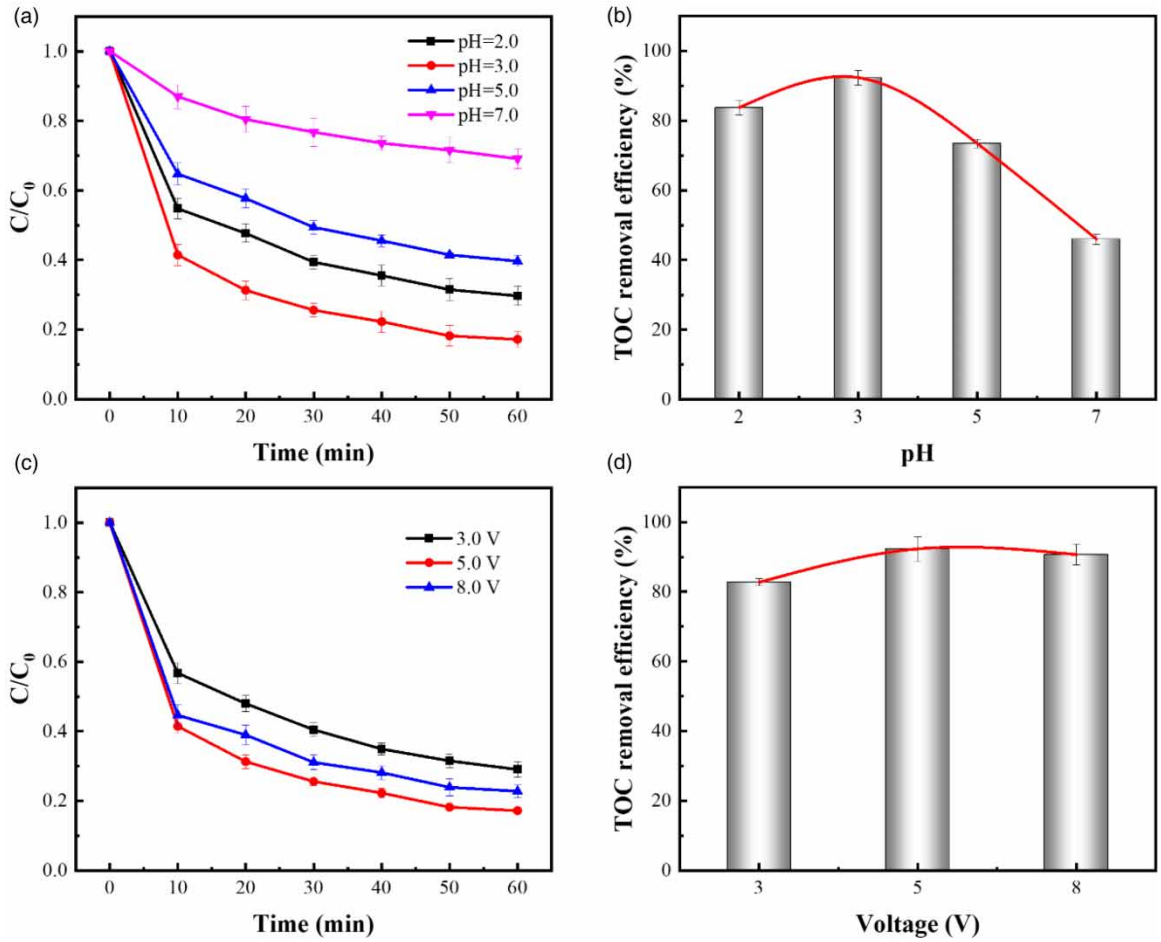

Figure 2 | Influence of different solution acidities on (a) COD and (b) TOC removal efficiencies; effect of different applied voltages on (c) COD and (d) TOC removal efficiencies.

enhanced electrode polarization and the occurrence of severe cathodic and anodic side reactions (Equation (12)) at higher applied voltage. The higher current causes a more violent side reaction of water electrolysis with byproduct O_2, which results in a decrease of ·OH (Zheng *et al.* 2018). As listed in Table S2, the energy consumption of the reaction at different voltages by Equation (9) also proves that a large amount of electrical energy will be consumed by the side reaction at a higher voltage. Here, 5.0 V was chosen as the appropriate voltage for this study. Under optimal conditions, the actual energy consumption required is 7.79 $kWhm^{-3}$, which is advantageous when compared with other methods for degrading actual wastewater (Table S4). In addition, the raw materials required for the experiment and the costs are briefly calculated in the supporting information (Table S3).

$$2H_2O \rightarrow O_2 + 4H^+ + 4e^- \tag{12}$$

3.2. Kinetics of COD removal by electro-Fenton process

The COD removal under various voltages was in accordance with the model of pseudo-first-order kinetic (Figure S2 and Table S5). The whole electro-Fenton process involved two different phases of rapid reaction and slow reaction, and the removal efficiency within the first 10 min was much greater than that in the latter stage within 1 h. In the fast reaction stage, a high concentration of H_2O_2 including the electrocatalytically generated H_2O_2 reacted with Fe^{2+} to produce more ·OH to rapidly degrade the dyeing pollutants. The lower efficiency in the later stage was caused by the fact that Fe^{3+} cannot be rapidly reduced to Fe^{2+} and the efficiency of ·OH generation decreases due to H_2O_2 consumption.

3.3. Electrochemical analysis

Tafel and Nyquist diagrams at different H_2O_2 concentrations were conducted to further investigate the electro-Fenton performance for the mineralization of textile wastewater (Figure 3). Potential window ranging from −1.2 to 1.2 V was set for Tafel curves. The corrosion potentials were measured as 0.21, −0.05 and 0.04 V for hydrogen peroxide concentrations of 0.15, 0.10 and 0.05, respectively. Obviously, the E_{corr} is much smaller than the values under other conditions at a hydrogen peroxide concentration of 0.10 mol·L^{-1} indicating the highest electrode activity for this electro-Fenton reaction. As the concentration is further increased, the critical value for the occurrence of the reaction increases and the E_{corr} moves in the positive direction, which is consistent with the previous analysis that the larger H_2O_2 concentration causes severe side reactions. The corrosion currents were 4.44, 1.63 and 3.76 mA at different H_2O_2 concentrations of 0.15, 0.10 and 0.05 mol·L^{-1}, respectively. Lower corrosion potential and corrosion current at 0.10 mol·L^{-1} of H_2O_2 concentration imply that easier anodic oxidation and slower anodic corrosion rate occurred, thus reducing the generation of iron sludge and making the Fe^{3+}/Fe^{2+} conversion more adequate. Nyquist plots showed that the interfacial transfer resistance (Rct) at different H_2O_2 concentrations (0.05, 0.10, 0.15 mol·L^{-1}) were 10.00, 7.32 and 9.07 Ω, respectively, with the smallest Rct value at 0.10 mol·L^{-1}, which is consistent with above observation that mZVI is more susceptible to anodic oxidation at 0.10 mol·L^{-1} of H_2O_2 concentration.

3.4. Reusability of anode material

Ti/RuO_2-IrO_2 flakes and mZVI powder are two important components of the composite anode. Herein, the utilization of mZVI powder in the electro-Fenton reaction at various initial pH values (Figure 4(a)) and the loss of Ti/RuO_2-IrO_2 flakes under multiple repetitions of the test were examined, respectively. First, the concentration of Fe^{2+} in the wastewater under neutral conditions was much smaller than that under acidic conditions. The Fe^{2+} concentration reached a maximum value at the initial pH = 3 after 60 min of reaction. In addition, the value of [DFe^{2+}]/[TDFe] at pH = 2.0 (8.4%) was significantly lower than that pH = 3.0 (38.9%). Obviously, the Fe^{2+} utilization at pH = 2.0 is low indicating that a large amount of hydrated ferric hydroxide would be produced after the reaction. Figure 4(b) presents the average TOC removal efficiency maintaining a value as high as 91.5% after five replicate experiments, indicating that the Ti/RuO_2-IrO_2 electrode was not effected during the experiments after simple washing with deionized water for each experiment. Therefore, the composite anode in this experiment is of low cost and good stability.

3.5. Characterization of precipitation

Iron-based precipitate flocs were formed in the textile wastewater after 60 min treatment via electro-Fenton process. The morphologic structure and chemical elements of the flocs were analyzed via SEM-EDS (Figure 5(a) and 5(b)). SEM shows that the precipitates are irregular spherical aggregates with a rough surface and spherical particles with a particle

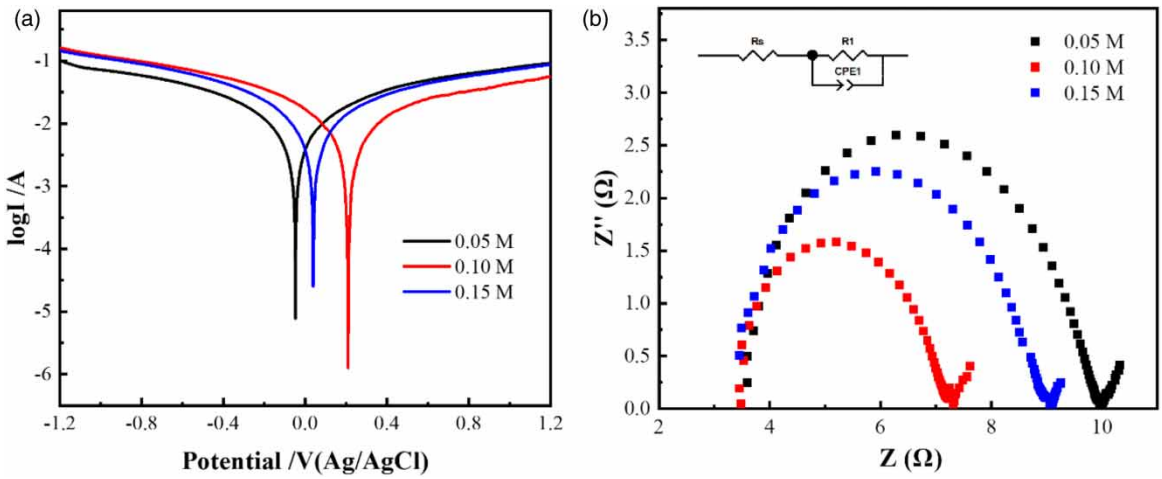

Figure 3 | (a) Tafel plots (b) Nyquist plots, of mZVI anode at various H_2O_2 concentrations. Reaction conditions: Pollutants = 200 mL; pH = 3.0; $[Fe]_0$ = 1.0 g·L^{-1}; Applied voltage = 5.0 V.

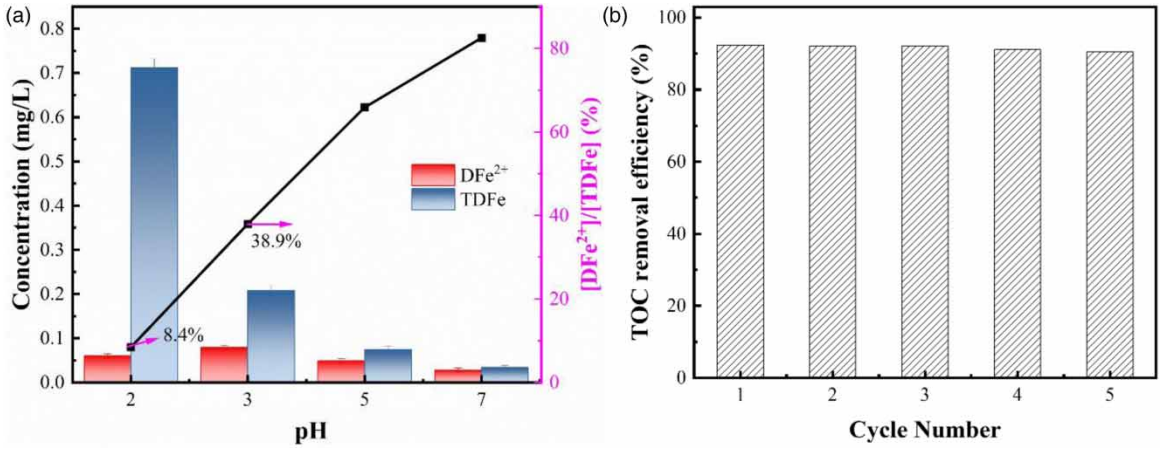

Figure 4 | (a) Utilization of mZVI at different initial pH; (b) Reusability of the anode material after five cycles of experiment. Reaction conditions: Pollutants = 200 mL; $[Fe]_0 = 1.0\ g{\cdot}L^{-1}$; $H_2O_2 = 2\ mol{\cdot}L^{-1}$; Applied voltage = 5.0 V.

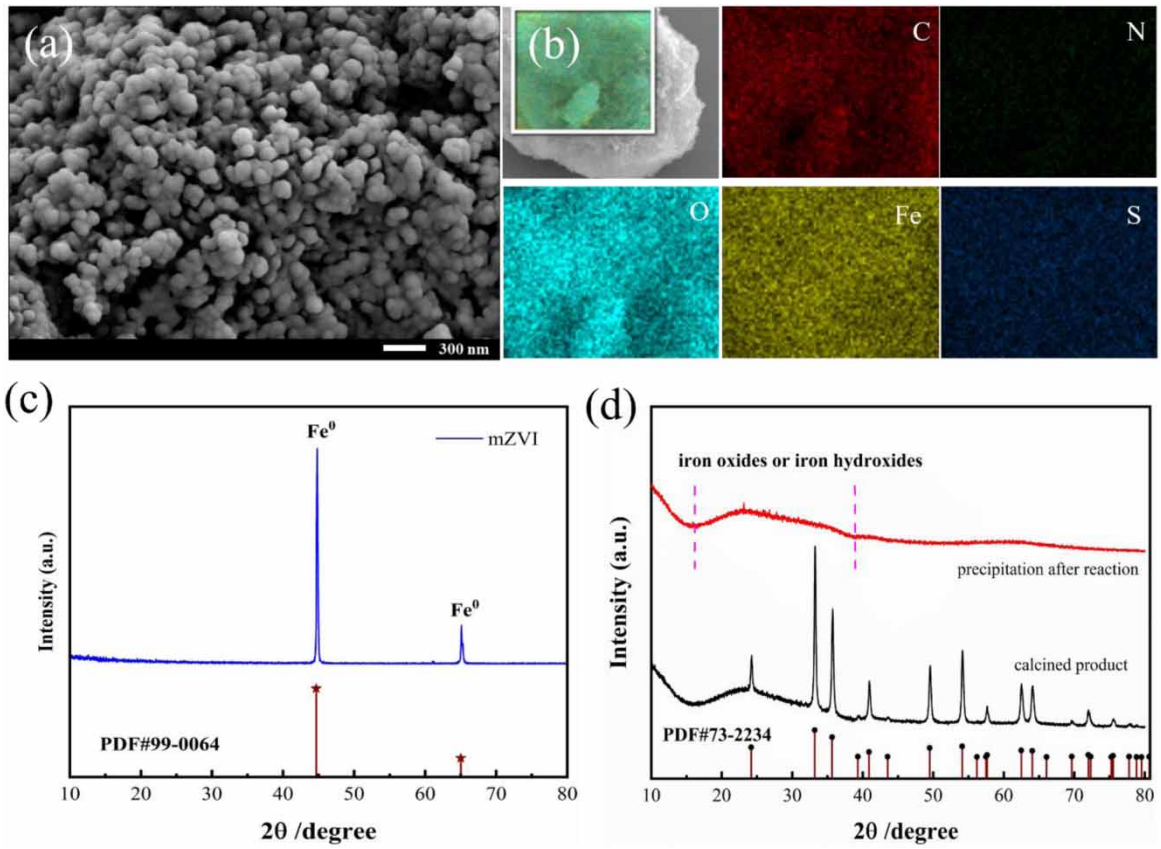

Figure 5 | Scanning electron microscopy images (a), element mappings (b) and XRD spectra (c,d) of mZVI and precipitate before and after calcination.

size of about 100 nm. Elemental mapping illustrated that the precipitates were composed of C (16.15 wt%), N (4.3 wt%), O (39.20 wt%), Fe (37.36 wt%) and S (2.99 wt%). The results indicate that the primary components of formed flocs precipitate are ferric oxides and ferric hydroxides (e.g. Fe_2O_3, Fe_3O_4, $Fe(OH)_2$, $Fe(OH)_3$ and FeO(OH)). A small amount of sulfur in the precipitate illustrates that the dyeing pollutants are partially removed by the flocculation. XRD analysis was performed on

mZVI before the reaction and the precipitate after the reaction to further investigate the composition of the precipitate (Figure 5(c)). However, the XRD patterns of the precipitated samples showed no characteristic peak of $Fe(OH)_3$ because the generated $Fe(OH)_3$ flocs were non-crystalline and therefore could not be readily measured by XRD analysis (Yoon *et al.* 2016). After calcination of the precipitate sample at 400 °C, eight major characteristic peaks of the XRD pattern were observed and well fitted with the standard card (PDF#73-2234) of iron oxide, which laterally proved that the precipitate were flocs of iron hydroxide.

Figure 6 displays the XPS spectra of the iron-based flocs precipitate. XPS survey spectrum shows the existence of carbon, oxygen, sulfur, nitrogen and iron elements in composition (Figure 6(a)). High-resolution core-level scans of the O 1s, C 1s and Fe 2p were also performed. Figure 6(b) demonstrates that the C 1s spectrum contains three main peaks with binding energies, corresponding to carbon–carbon single bond (C-C, 284.5 eV) and carbon–carbon double bond (C = C, 286.5 eV) bonds and carbon–oxygen double bond (C = O, 288.4 eV), respectively, which indicates that the dye pollutants removal process is based on synergistic effects involving dominant degradation and partial flocs adsorption (Mattevi *et al.* 2009). Three intense peaks are observed at 529.8, 531.3 and 532.2 eV in the O 1s spectrum (Figure 6(c)). The O1s peak located at 529.7–530.1 eV corresponds to oxygen (O^{2-}) on the basis of the report by Piumetti *et al.* The peak with a binding energy of 531.3 eV belongs to the surface adsorbed oxygen (OH^-) and the binding energy at 532.2 eV can be attributed to the physical or chemical adsorption of water (H_2O) (Sun *et al.* 2020). Furthermore, the peak position of Fe $2p_{3/2}$ is between 710.6 and 711.2 eV, and Fe $2p_{1/2}$ is located in 723.2–724.8 eV (Yamashita & Hayes 2008; Do *et al.* 2013). In this study, the

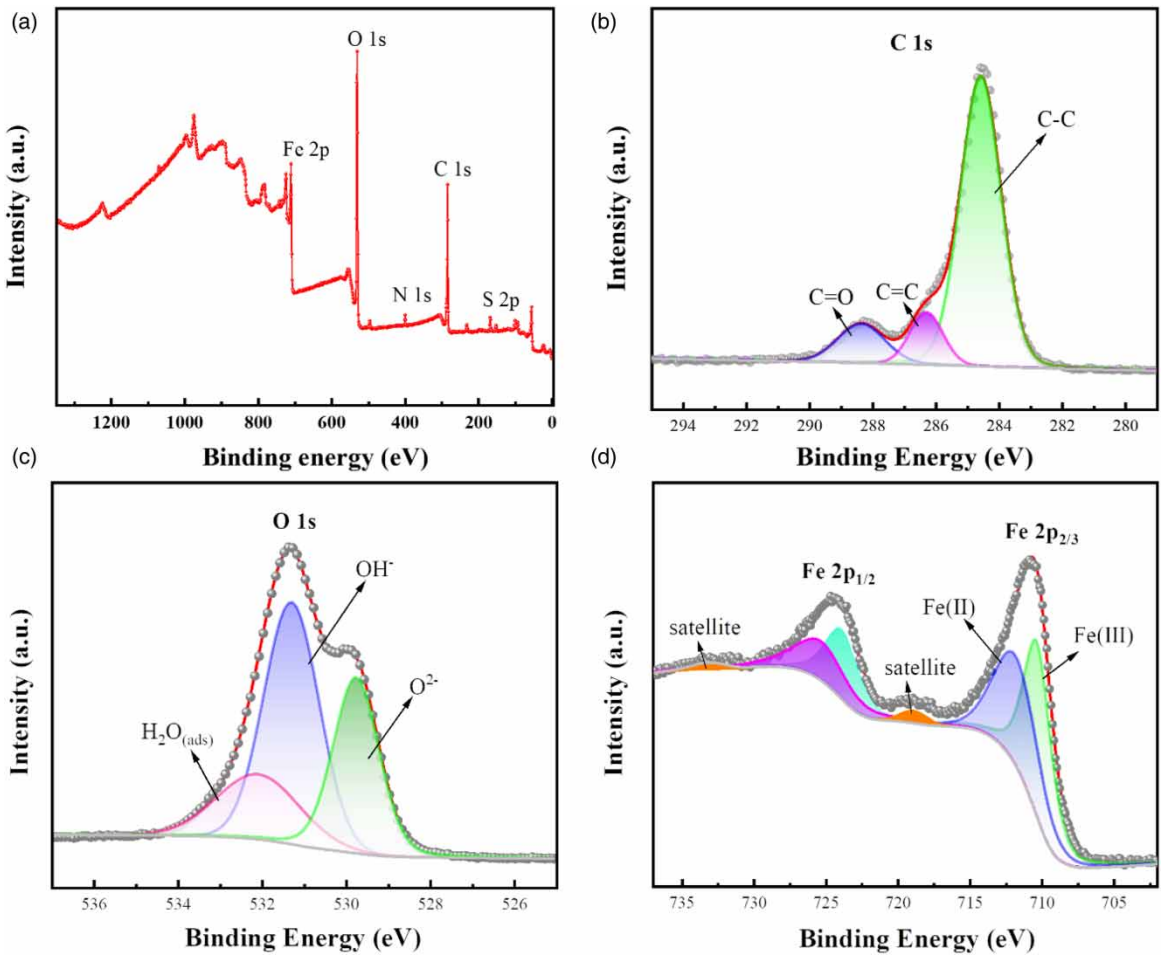

Figure 6 | XPS survey spectra of the flocs precipitate from Electro-Fenton process, (a) survey spectrum, (b) high-resolution C 1 s core level, (c) O 1 s core level and (d) Fe 2p core level.

Fe 2p spectrum includes characteristic peaks at 710.8 and 724.5 eV, corresponding to the Fe $2p_{3/2}$ and Fe $2p_{1/2}$ states, respectively (Figure 6(d)). The peak at 710.5 eV implies the presence of the ferric state in Fe_2O_3 (Kumar *et al.* 2015). The peak located at 712.2 eV is ferrous iron of Fe_3O_4. In summary, the ferrous compounds in the flocs precipitate can be classified into iron hydroxide (i. e. $Fe(OH)_2$, $Fe(OH)_3$ and FeO(OH)) and iron oxide (i. e. Fe_2O_3 and Fe_3O_4). The existence of low intensity of N and S implies that N, S-containing organics were degraded and marginally adsorbed on the flocs, which is supported by the evidence of little increase of the sulfate and nitrate concentration in wastewater during electro-Fenton reaction.

3.6. Degradation mechanism

GC-MS analysis on treated and untreated real textile wastewater was performed to investigate the degradation mechanism. The results are presented in Table S6 and the corresponding mass spectra are listed in the supporting information (Figure S4). These include amide compounds, ester auxiliaries, polysiloxanes and halogen-containing flame retardants. Among them, the amide compounds are effective in improving the surface dyeing depth of the dyed and finished fabrics and improving their deficiencies in color light shading, resulting in a much higher surface depth and color fixation rate of the fabrics. Polysiloxane has excellent flexibility, thermal stability and chemical stability. In the textile process, it is normally used in the co-condensation of polysiloxane into the co-polyester molecular chain, reducing the dyeing temperature of blended fibers to avoid high temperature and high voltage dyeing technology on the blended fiber damage. Evidently, the GC-MS analysis proved that the large molecules containing benzene ring and other hard-to-degrade pollutants were opened to form aliphatic hydrocarbons and then further degraded to small molecules with a high mineralization rate during the electro-Fenton degradation process. However, slight ester pollutants were still detected at the end of the degradation reaction, which may be caused by the complexity of the actual wastewater and the acidic environment even after the reaction unfavorable for esters degradation. Therefore, the high efficiency of this electro-Fenton can be considered a pre-treatment process to achieve a cost-effective treatment of dyeing wastewater.

The plausible degradation mechanism of the electro-Fenton reaction is illustrated in Figure 7. The combination of Fe^{2+} from the anode dissolution and H_2O_2 generated on the cathode produces ·OH to degrade pollutants, which are mineralized or partially mineralized into CO_2 and H_2O and other inorganic ions. At the same time, Fe^{2+}/Fe^{3+} reduction occurs at the cathode under the electric field, allowing the Fenton reaction to circulate. In addition, iron ions are electro-dissoluted into the wastewater to produce iron hydroxides as coagulants, which adsorb colloidal or soluble pollutants for further pollutant removal.

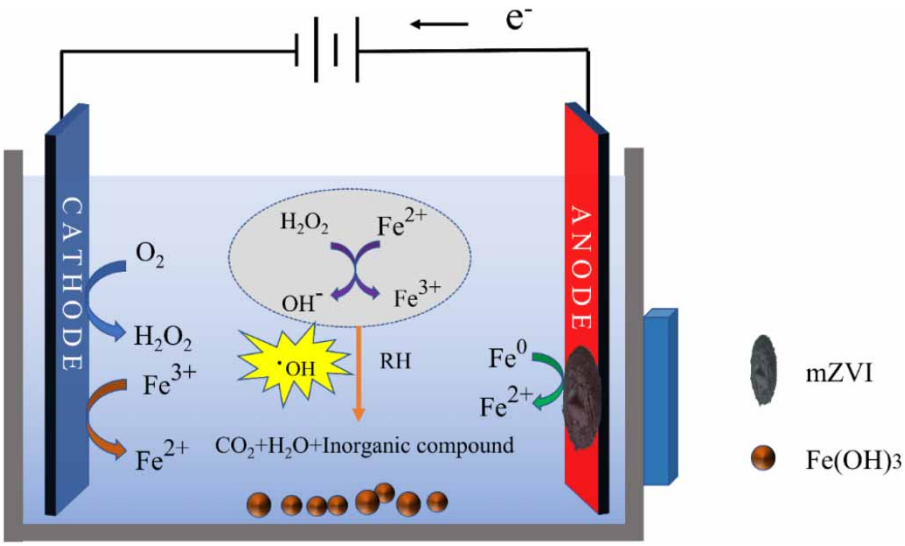

Figure 7 | Rational mechanism of electro-Fenton reaction under optimum conditions.

4. CONCLUSIONS

In this study, we investigated the mineralization of real textile wastewater by novel heterogeneous E-Fention with a composite anode composed of magnetically fixed mZVI and RuO_2-IrO_2-Ti sheets. The specific degradation efficiencies were studied under different parameters on the basis of COD and TOC removal. It was demonstrated that the COD and TOC removal efficiencies of 82.84 and 92.44%, respectively, could be achieved at an mZVI loading of 1.0 $g{\cdot}L^{-1}$, an H_2O_2 concentration of 0.10 $mol{\cdot}L^{-1}$, a load voltage of 5.0 V and an initial pH of 3.0 within 60 min. This high mineralization efficiency was supported by the GC-MS investigation according to the types of pollutants. Several main pollutants in raw wastewater (amides, ester additives, polysiloxane and halogenated flame retardants, etc.) are degraded into small molecules and completely removed. The removal efficiencies of COD follow a pseudo primary kinetic model. The whole electro-Fenton removal process was divided into two stages: fast reaction and slow reaction. In addition, the physico-chemical analysis of precipitate by EDS and XPS proved that the precipitate was iron oxide/iron hydroxide, which could be used as a coagulant to further remove the pollutants. The mZVI-based electro-Fenton system has a high $[DFe^{2+}]$/[TDFe] value with an excellent electrochemical performance. In summary, this study showed that RuO_2-IrO_2/mZVI-Ti anode can effectively be employed in the electro-Fenton reaction to treat real textile wastewater.

ACKNOWLEDGEMENT

We acknowledge the financial support for this work provided by Open Foundation of State Environmental Protection Key Laboratory of Mineral Metallurgical Resources Utilization and Pollution Control (HB201909). Authors have full power to use these grants.

DATA AVAILABILITY STATEMENT

All relevant data are included in the paper or its Supplementary Information.

CONFLICT OF INTEREST

The authors declare there is no conflict.

REFERENCES

Baddouh, A., El Ibrahimi, B., Rguitti, M. M., Mohamed, E., Hussain, S. & Bazzi, L. 2019a Electrochemical removal of methylene bleu dye in aqueous solution using Ti/RuO_2–IrO_2 and SnO2 electrodes. *Separation Science and Technology* **55**, 1852–1861. doi:10.1080/01496395.2019.1608244.

Baddouh, A., El Ibrahimi, B., Amaterz, E., Oukhrib, R. & Bazzi, L. 2019b Removal of the rhodamine B Dye at Ti/Ru0.3Ti0.7O_2 anode using flow cell system. *Journal of Chemistry* **2019**, 1–10. doi:10.1155/2019/1424797.

Baddouh, A., El Ibrahimi, B., Amaterz, E., Oukhrib, R. & Bazzi, L. 2022 Using Ti/Ti0.7Ru0.3O_2 anode-type with a flow cell system for the electrochemical treatment of a tannery wastewater. *Ozone: Science & Engineering* 1–13. doi:10.1080/01919512.2022.2124953.

Bahadur, N. & Bhargava, N. 2019 Novel pilot scale photocatalytic treatment of textile & dyeing industry wastewater to achieve process water quality and enabling zero liquid discharge. *Journal of Water Process Engineering* **32**. doi:10.1016/j.jwpe.2019.100934.

Bakheet, B.Yuan, S., Li, Z., Wang, H., Zuo, J., Komarneni, S. & Wang, Y. 2013 Electro-peroxone treatment of Orange II dye wastewater. *Water Research* **47**, 6234–6243. doi:10.1016/j.watres.2013.07.042.

Bilińska, L., Gmurek, M. & Ledakowicz, S. 2017 Textile wastewater treatment by AOPs for brine reuse. *Process Safety and Environmental Protection* **109**, 420–428. doi:10.1016/j.psep.2017.04.019.

Bilinska, L., Blus, K., Foszpanczyk, M., Gmurek, M. & Ledakowicz, S. 2020 Catalytic ozonation of textile wastewater as a polishing step after industrial scale electrocoagulation. *Journal of Environmental Management* **265**, 110502. doi:10.1016/j.jenvman.2020.110502.

Bolton, J. R., Bircher, K. G. & Tumas, W. 2001 Figures of merit for the technical development and application of advanced oxidation technologies for both electric-and solar-driven systems. *Pure and Applied Chemistry* **73**, 627–637.

Cai, M., Su, J., Lian, G., Wei, X., Dong, C., Zhang, H., Jin, M. & Wei, Z. 2016 Sono-advanced Fenton decolorization of azo dye Orange G: analysis of synergistic effect and mechanisms. *Ultrason Sonochem* **31**, 193–200. doi:10.1016/j.ultsonch.2015.12.017.

Chen, Q., Yang, Y., Zhou, M., Liu, M., Yu, S. & Gao, C. 2015 Comparative study on the treatment of raw and biologically treated textile effluents through submerged nanofiltration. *Journal of Hazardous Materials* **284**, 121–129. doi:10.1016/j.jhazmat.2014.11.009.

Chow, C.-H. & Leung, K. S.-Y. 2019 Removing acesulfame with the peroxone process: transformation products, pathways and toxicity. *Chemosphere* **221**, 647–655. doi:10.1016/j.chemosphere.2019.01.082.

Do, S.-H., Kwon, Y.-J., Bang, S.-J. & Kong, S.-H. 2013 Persulfate reactivity enhanced by Fe_2O_3–MnO and CaO–Fe_2O_3–MnO composite: identification of composite and degradation of CCl_4 at various levels of pH. *Chemical Engineering Journal* **221**, 72–80. doi:10.1016/j.cej.2013.01.097.

Dolatabadi, M., Ghaneian, M. T., Wang, C. & Ahmadzadeh, S. 2021 Electro-Fenton approach for highly efficient degradation of the herbicide 2,4-dichlorophenoxyacetic acid from agricultural wastewater: process optimization, kinetic and mechanism. *Journal of Molecular Liquids* **334**. doi:10.1016/j.molliq.2021.116116.

Feng, Y., Yang, L., Liu, J. & Loga, B. E. 2016 Electrochemical technologies for wastewater treatment and resource reclamation. *Environmental Science: Water Research & Technology* doi:10.1039/C5EW00289C.

Fu, F., Dionysiou, D. D. & Liu, H. 2014 The use of zero-valent iron for groundwater remediation and wastewater treatment: a review. *Journal of Hazardous Materials* **267**, 194–205. doi:10.1016/j.jhazmat.2013.12.062.

Ghalebizade, M. & Ayati, B. 2019 Acid Orange 7 treatment and fate by electro-peroxone process using novel electrode arrangement. *Chemosphere* **235**, 1007–1014. doi:10.1016/j.chemosphere.2019.06.211.

Huang, Y., Jiang, J., Ma, L., Wang, Y., Liang, M., Zhang, Z. & Li, L. 2020 Iron foam combined ozonation for enhanced treatment of pharmaceutical wastewater. *Environmental Research* **183**, 109205. doi:10.1016/j.envres.2020.109205.

Ileri, B. & Dogu, I. 2022 Sono-degradation of Reactive Blue 19 in aqueous solution and synthetic textile industry wastewater by nanoscale zero-valent aluminum. *Journal of Environmental Management* **303**, 114200. doi:10.1016/j.jenvman.2021.114200.

Ju, Y., Li, H., Wang, Z., Liu, H., Huo, S., Jiang, S., Duan, S., Yao, Y., Lu, X. & Chen, F. 2022 Solar-driven on-site H_2O_2 generation and tandem photo-Fenton reaction on a triphase interface for rapid organic pollutant degradation. *Chemical Engineering Journal* **430**. doi:10.1016/j.cej.2021.133168.

Kaur, P., Kushwaha, J. P. & Sangal, V. K. 2018 Electrocatalytic oxidative treatment of real textile wastewater in continuous reactor: degradation pathway and disposability study. *Journal of Hazardous Materials* **346**, 242–252. doi:10.1016/j.jhazmat.2017.12.044.

Kenova, T. A., Kornienko, G. V., Golubtsova, O. A., Kornienko, V. L. & Maksimov, N. G. 2018 Electrochemical degradation of Mordant Blue 13 azo dye using boron-doped diamond and dimensionally stable anodes: influence of experimental parameters and water matrix. *Environmental Science and Pollution Research* **25**, 30425–30440. doi:10.1007/s11356-018-2977-z.

Khataee, A. R., Safarpour, M., Zarei, M. & Aber, S. 2011 Electrochemical generation of H_2O_2 using immobilized carbon nanotubes on graphite electrode fed with air: investigation of operational parameters. *Journal of Electroanalytical Chemistry* **659**, 63–68. doi:10.1016/j.jelechem.2011.05.002.

Khlifi, R., Belbahri, L., Woodward, S., Ellouz, M., Dhouib, A., Sayadi, S. & Mechichi, T. 2010 Decolourization and detoxification of textile industry wastewater by the laccase-mediator system. *Journal of Hazardous Materials* **175**, 802–808. doi:10.1016/j.jhazmat.2009.10.079.

Kishor, R., Purchase, D., Saratale, G. D., Saratale, R. G., Ferreira, L. F. R., Bilal, M., Chandra, R. & Bharagava, R. N. 2021 Ecotoxicological and health concerns of persistent coloring pollutants of textile industry wastewater and treatment approaches for environmental safety. *Journal of Environmental Chemical Engineering* **9**. doi:10.1016/j.jece.2020.105012.

Kumar, S., Prakash, R., Choudhary, R. J. & Phase, D. M. 2015 Structural, XPS and magnetic studies of pulsed laser deposited Fe doped Eu_2O_3 thin film. *Materials Research Bulletin* **70**, 392–396. doi:10.1016/j.materresbull.2015.05.007.

Li, Y., Liu, L., Zhang, Q., Su, Y. & Zhou, M. 2021 Hybrid electro-Fenton and peroxi-coagulation process for high removal of 2,4-dichlorophenoxiacetic acid with low iron sludge generation. *Electrochimica Acta* **382**. doi:10.1016/j.electacta.2021.138304.

Liu, H. & Wang, C. 2007 A novel electro-Fenton process for water treatment: reaction-controlled pH adjustment and performance assessment. *Environmental Science & Technology* **41**, 2937–2942. doi:10.1021/es0622195.

Martínez-Huitle, C. A. & Brillas, E. 2009 Decontamination of wastewaters containing synthetic organic dyes by electrochemical methods: a general review. *Applied Catalysis B: Environmental* **87**, 105–145. doi:10.1016/j.apcatb.2008.09.017.

Mattevi, C., Eda, G., Agnoli, S., Miller, S., Mkhoyan, K. A., Celik, O., Mastrogiovanni, D., Granozzi, G., Garfunkel, E. & Chhowalla, M. 2009 Evolution of electrical, chemical, and structural properties of transparent and conducting chemically derived graphene thin films. *Advanced Functional Materials* **19**, 2577–2583. doi:10.1002/adfm.200900166.

Naje, A. S., Chelliapan, S., Zakaria, Z., Ajeel, M. A. & Alaba, P. A. 2017 A review of electrocoagulation technology for the treatment of textile wastewater. *Reviews in Chemical Engineering* **33**. doi:10.1515/revce-2016-0019.

Nakhate, P. H., Gadipelly, C. R., Joshi, N. T. & Marathe, K. V. 2019 Engineering aspects of catalytic ozonation for purification of real textile industry wastewater at the pilot scale. *Journal of Industrial and Engineering Chemistry* **69**, 77–89. doi:10.1016/j.jiec.2018.09.010.

Nidheesh, P. V. & Gandhimathi, R. 2012 Trends in electro-Fenton process for water and wastewater treatment: an overview. *Desalination* **299**, 1–15. doi:10.1016/j.desal.2012.05.011.

Pan, Z.-l. & Qian, X.-f. 2022 Porous carbons for use in electro-Fenton and Fenton-like reactions. *New Carbon Materials* **37**, 180–195. doi:10.1016/s1872-5805(22)60578-x.

Paz, A., Carballo, J., Perez, M. J. & Dominguez, J. M. 2017 Biological treatment of model dyes and textile wastewaters. *Chemosphere* **181**, 168–177. doi:10.1016/j.chemosphere.2017.04.046.

Paździor, K., Bilińska, L. & Ledakowicz, S. 2019 A review of the existing and emerging technologies in the combination of AOPs and biological processes in industrial textile wastewater treatment. *Chemical Engineering Journal* **376**, 120597. doi:10.1016/j.cej.2018.12.057.

Pignatello, J. J., Oliveros, E. & MacKay, A. 2006 Advanced oxidation processes for organic contaminant destruction based on the Fenton reaction and related chemistry. *Critical Reviews in Environmental Science and Technology* **36**, 1–84. doi:10.1080/10643380500326564.

Pulgarin, C., Adler, N., Péringer, P. & Comninellis, C. 1994 Electrochemical detoxification of a 1,4-benzoquinone solution in wastewater treatment. *Water Research* **28**, 887–893. doi:10.1016/0043-1354(94)90095-7.

Samuchiwal, S., Gola, D. & Malik, A. 2021 Decolourization of textile effluent using native microbial consortium enriched from textile industry effluent. *Journal of Hazardous Materials* **402**, 123835. doi:10.1016/j.jhazmat.2020.123835.

Santos, D. H. S., Duarte, J. L. S., Tavares, M. G. R., Tavares, M. G., Friedrich, L. C., Meili, L., Pimentel, W. R. O., Tonholo, J. & Zanta, C. L. P. S. 2020 Electrochemical degradation and toxicity evaluation of reactive dyes mixture and real textile effluent over DSA® electrodes. *Chemical Engineering and Processing – Process Intensification* **153**. doi:10.1016/j.cep.2020.107940.

Sarikaya, R., Selvi, M. & Erkoc, F. 2012 Evaluation of potential genotoxicity of five food dyes using the somatic mutation and recombination test. *Chemosphere* **88**, 974–979. doi:10.1016/j.chemosphere.2012.03.032.

Sayin, F. E., Karatas, O., Ozbay, I., Gengec, E. & Khataee, A. 2022 Treatment of real printing and packaging wastewater by combination of coagulation with Fenton and photo-Fenton processes. *Chemosphere* **306**, 135539. doi:10.1016/j.chemosphere.2022.135539.

Somensi, C. A., Simionatto, E. L., Bertoli, S. L., Wisniewski Jr., A. & Radetski, C. M. 2010 Use of ozone in a pilot-scale plant for textile wastewater pre-treatment: physico-chemical efficiency, degradation by-products identification and environmental toxicity of treated wastewater. *Journal of Hazardous Materials* **175**, 235–240. doi:10.1016/j.jhazmat.2009.09.154.

Sun, D., Hong, X., Cui, Z., Du, Y., Hui, K. S., Zhu, E., Wu, K. & Hui, K. N. 2020 Treatment of landfill leachate using magnetically attracted zero-valent iron powder electrode in an electric field. *Journal of Hazardous Materials* **388**, 121768. doi:10.1016/j.jhazmat.2019.121768.

Yamashita, T. & Hayes, P. 2008 Analysis of XPS spectra of Fe2 + and Fe3 + ions in oxide materials. *Applied Surface Science* **254**, 2441–2449. doi:10.1016/j.apsusc.2007.09.063.

Yamjala, K., Nainar, M. S. & Ramisetti, N. R. 2016 Methods for the analysis of azo dyes employed in food industry–A review. *Food Chemistry* **192**, 813–824. doi:10.1016/j.foodchem.2015.07.085.

Yoon, I.-H., Yoo, G., Hong, H.-J., Kim, J., Kim, M. G., Choi, W.-K. & Yang, J.-W. 2016 Kinetic study for phenol degradation by ZVI-assisted Fenton reaction and related iron corrosion investigated by X-ray absorption spectroscopy. *Chemosphere* **145**, 409–415. doi:10.1016/j.chemosphere.2015.11.108.

Zheng, H.-S., Guo, W.-Q., Wu, Q.-L., Ren, N.-Q. & Chang, J.-S. 2018 Electro-peroxone pretreatment for enhanced simulated hospital wastewater treatment and antibiotic resistance genes reduction. *Environment International* **115**, 70–78. doi:10.1016/j.envint.2018.02.043.

First received 9 November 2022; accepted in revised form 18 January 2023. Available online 3 February 2023